processes

MDPI

Article

Influence of 12Cr1MoV Material on Tissue Properties at High Temperature and Long Operating Time

Jiawei Liu and Yuanzhe Li *

School of Materials Science & Engineering, Nanyang Technological University, Singapore 639798, Singapore; l92j07w10@163.com

* Correspondence: yuanzhe001@e.ntu.edu.sg

Abstract: 12Cr1MoV is commonly used for pressure pipes in thermal power plants. However, its service life has always prevented the development of such metallic materials. This experiment applies a tensile and impact experiment to investigate the metal cluster of 12Cr1MoV low-alloy and heat-resistant steel with 60,000 h service at 550 °C. Results indicate that, after 60,000 h of high-temperature exposure, the metal cluster of Cr, Mo, and V elements may gradually decrease. First, the decreasing elements will precipitate out of the solid solution. Then, the precipitated elements transform into carbides that accumulate and grow on the grain boundaries. The continuous growth of the precipitated carbide of alloy elements may also create pearlite in the cluster, which results in severe pearlite periodization and tensile fracture due to plastic, through-crystal fracture. Then, the solid solution-strengthened tissue disappears, which severely decreases the thermal strength of 12Cr1MoV low-alloy and heat-resistant steel. At the same time, the brittleness of the steel will increase. The end of life of the metal occurs after 60,000 h of high-temperature use at 550 °C. This result may also provide a basis for future life assessment of 12Cr1MoV steel.

Keywords: 12Cr1MoV; high temperatures and long operating times; carbide precipitation phase; solid solution strengthening

Citation: Liu, J.; Li, Y. Influence of 12Cr1MoV Material on Tissue Properties at High Temperature and Long Operating Time. *Processes* **2022**, *10*, 192. https://doi.org/10.3390/pr10020192

Academic Editor: Andrea Petrella

Received: 24 December 2021
Accepted: 18 January 2022
Published: 19 January 2022

1. Introduction

As industries develop increasingly complex processes, metal industrial pipes are developed to last longer under higher temperatures and pressures. For example, between 1950 and 1960, thermal power plants often used Q235 steel for steam pipes that operate at temperatures of about 270 °C. However, between 1960 and 1980, most thermal power plants used Cr-Mo steel for steam pipes at temperatures of about 400 °C. Then, between 1980 and 2000, most thermal power plants used Cr-Mo-V steel for steam pipes that operate at about 530 °C [1]. Currently, thermal power generating units operate at 630 °C and the pipes are of SA335-P92 steel.

In the 1970s, the Soviet Union developed 12X1MØ, a binary chromium–molybdenum steel that is heat-resistant, ternary, or low-alloyed, with reduced chromium content and 0.25% more vanadium [1,2]. In the 1990s, China improved the 12X1MØ manufacturing process and created 12CrMoV steel [1,3] with added vanadium that formed the VC carbide and improved the thermal strength of 12CrMoV steel from 540 °C to 560 °C [1,4]. In comparison, 2Cr1Mo steel and 15CrMo steel have a thermal strength of 550 °C. Moreover, manufacturers in China increased chromium content by 1% to improve the thermal strength of 12CrMoV steel. As a result, this is the steel grade that is widely used in Chinese power station boiler components such as steam pipes, where steam parameters do not exceed 540 °C.

Before use, 12Cr1MoV steel is in a normalized plus tempered condition with a ferrite plus pearlite metallographic cluster. When 12CrMoV steel is used over the long term at high temperatures, periodization occurs in the pearlite of the metals. In other words, after

200,000 h of use, the cementite in the pearlite gradually changes to granular carbide and the mechanical properties of 12CrMoV steel deteriorate by 90%. To ensure safety in this scenario, the equipment needs to be replaced [5].

At the same time, the wide variety of industrial uses of metal materials means that different metals subjected to different conditions for different lengths of time result in different deterioration patterns and remaining lifetimes. Meanwhile, there are no comprehensive international standards for the assessment of the life of metals. For instance, the American Society of Mechanical Engineers (ASME-SA335/SA335M) standard only determines whether the metals pass or fail in a particular aspect. The current international approach to material life assessment is homogeneous. In practical engineering applications, material life is evaluated in a macroscopic way by analyzing the mechanical properties of the material. However, scientific research units are inclined to analyze the microstructure of materials to determine the life of materials. Fewer studies have been carried out to assess material life by linking the macroscopic mechanical properties and microstructure of materials.

To provide a basis for the assessment of creep damage and life assessment of 12Cr1MoV steel, this study evaluates the properties and microstructure of 12Cr1MoV steel that has been in use for at least 60,000 h. In this paper, the macroscopic mechanical properties and microstructure of 12Cr1MoV steel operating for 60,000 h are investigated. For the first time, the damage of 12Cr1MoV steel is analyzed by linking the macroscopic mechanical properties of the tissue to metallography as well as using scanning electron microscopy analysis. This study aims to provide a more accurate assessment of creep damage and remaining life, as reflected in three research goals: (a) to determine tissue state and distribution in 12Cr1MoV steel, (b) to analyze their intrinsic connections with the service aging of 12Cr1MoV steel, and (c) to evaluate the microstructure and property changes of 12Cr1MoV steel after long-term use.

Finally, this study presents the elicited database as well as a theoretical model for the future development of life assessment models for 12Cr1MoV steel [6–8].

2. Materials and Methods

2.1. Materials and Devices

The test 12Cr1MoV steel samples are selected from the same manufacturer (SMC, Shanghai, China), from the same batch of 12Cr1MoV steel pipe. For comparison and analysis, the control groups (Sample 1) consist of a new and unused 12Cr1MoV tube in a boiler plant stored in the spare parts store; Sample 2 consists of an industrial 12Cr1MoV sampling tube that had been in operation for 60,000 h in the ultra-supercritical unit of a 2 × 660 MW power plant in a low temperature reheater. The steam of around 40 bar for Sample 2 is heated to even above the main steam temperature at 590 °C. The temperature at the outlet of the reheater has to be maintained within a narrow band (580–590 °C).

2.2. Method of Analysis

Firstly, the chemical and morphological characterizations of new 12Cr1MoV tubes and 12Cr1MoV sampling tubes with 60,000 h of operation were analyzed using a scanning electron microscope (SEM) (Hitachi S-4700, Long Beach, CA, USA) that was attached to a Bruker AXS Quantax 4010 energy-dispersive X-ray spectrometer (EDX, Karlsruhe, Germany). Determination of the fluorescence intensity of carbon, manganese, chromium, molybdenum, vanadium, phosphorus, and other elements was performed using X-ray fluorescence spectrometry. Using the software that comes with the instrument, the curves are matrix corrected and spectral interference corrected to obtain specific values. For metallographic analysis, the tubes are made into metallographic specimens using resin and then surface etched using a 5% nitric acid-alcohol solution. We observed the metallographic microstructure after 5–9 s of etching with a corrosive.

Room temperature and 550 °C tensile properties tests were conducted on a 60,000-h run of 12Cr1MoV steel sampling tubes and new 12Cr1MoV tubes in the supplied condition

on a SANS CMT5205 electronic tensile tester. All samples were machined according to the ISO 148:2016 standard. Tensile and impact specimens were machined according to the ISO 6892–1:2016 standard and compared with GB5310-2008 to simulate actual operating conditions. Room temperature impact performance tests were performed on the RKP450 Pendulum Oscillation Impact Tester. In this study, the mean value of the best-fit distribution is used for the characteristic value of 12Cr1MoV steels. The 5th percentile value with 75% confidence level from test results shall be the characteristic value for their mechanical strengths. The fracture characteristics of 12Cr1MoV steel impact specimens run for 60,000 h were analyzed using a Tescon VEGA 3 LMU scanning electron microscope, and the precipitates from 12Cr1MoV steel sampling tubes run for 60,000 h were analyzed by energy spectrometry using an Oxford X-act [9]. Besides, the samples were cut into full-size specimens (10 mm × 10 mm) and tested via Teclock GS-709 N durometer type-A according to ASTM-D-2240. Measurements were acquired five times for each sample to get the average value with a short contact time of 1.0 s. Fracture analysis was carried out using scanning electron microscopy on the fracture area after the impact test.

3. Results and Discussions

3.1. Histochemical Analysis of Metals

First, the chemical composition of Sample 1 and Sample 2 was analyzed. Table 1 shows the results. Since the ASME standard only specifies the elemental content of P11, the results of this test also refer to the Chinese standard (GB5310-2008) for the elemental content of the steel grade 12Cr1MoV. Results indicate that the increase in high-temperature service time gradually decreases the content of Cr, Mo, and V elements in the metal structure.

Table 1. Sample 1 and Sample 2 chemical analysis results mass (%).

Type of Element	Mn	C	Si	Cr	Mo	V	Ni	S	P	Cu
Sample 1 content elements (%)	0.62	0.13	0.27	1.12	0.30	0.16	0.08	0.019	0.008	0.07
Sample 2 content elements (%)	0.60	0.15	0.27	0.97	0.26	0.11	0.07	0.017	0.009	0.05
ASME Standards Range (P11)	0.30–0.60	0.05–0.15	0.50–1.00	1.00–1.50	0.65–1.44	-	-	≤0.025	≤0.025	-
Scope of GB5310-2008 standard (12Cr1MoV)	0.40–0.70	0.08–0.15	0.17–0.37	0.90–1.20	0.25–0.35	0.15–0.30	≤0.30	≤0.03	≤0.03	≤0.20

The main role of the element Cr in the metal structure is to improve the stability and corrosion resistance of the matrix structure. The elements Mo and V are mainly used for solid solution strengthening. Tang et al., (2019) showed that, as the content of Cr, Mo, and V elements in the tissue decreased, the corrosion resistance and strength of the metal tissue decreased [4].

3.2. Metallographic Analysis

Figure 1a–c indicate the different positions of the original metallographic organization of 12Cr1MoV steel as well as the interface between 12Cr1MoV steel ferrite and pearlite in Sample 1. The new 12Cr1MoV steel requires normalizing with tempering heat treatment. The normal original organization of the new 12Cr1MoV steel is ferrite plus partial bainite or pearlite [10]. In the normal original organization of 12Cr1MoV steel, ferrite and pearlite should be uniformly distributed. There should be no bias in the composition of the steel, and there should be no carburization or metal inclusions that could harm the organization. A new 12Cr1MoV metallographic cluster was analyzed using the area method to calculate the ferrite area fraction of the polished surface of the metallographic, 55–67%, the pearlite area fraction of 30–42%, and the original carbide and non-metallic inclusions area fraction of 3–4.7% [10].

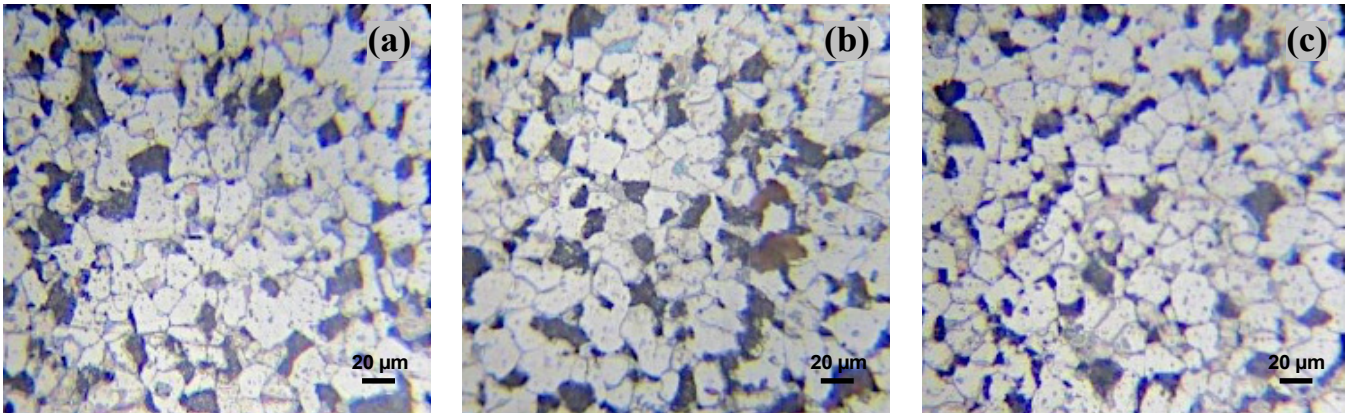

Figure 1. (**a**–**c**) normal original metallographic organization of 12Cr1MoV steel at different locations.

Figure 2 shows the metallographic organization of Sample 2. A large number of pearlite spheroidization can be observed within the figure. The metallographic organization is ferrite and some pearlite and bainite (red rectangular). There are also some carbide aggregates on the grain boundaries (blue rectangular) that tend to grow into grade 4.5 pearlite spheroids. For instance, test results show that, under long-term high temperature and high pressure, the carburized body in the pearlite organization begins to show spheroidization (red circled). At the same time, the ferrite begins to precipitate carbide within the matrix due to the reduction in Cr, Mo, and V elements in their solid solution. As service time increases, the carbide particles increase in size, which leads to the deterioration of the steel's ability to operate under high temperatures [11]. These results corroborate the results of the chemical composition analysis and the high-temperature tensile test.

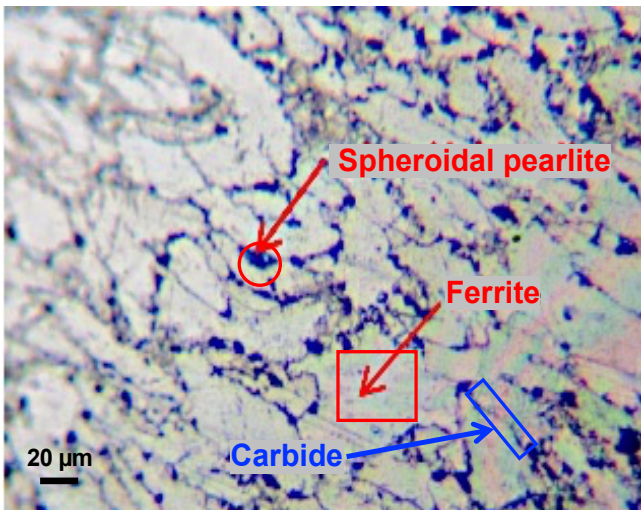

Figure 2. Metallographic organization of 12Cr1MoV steel running for 60,000 h.

The arrows within Figure 3a,b show a degree of precipitation on the along-crystal cracks in the SEM as well as metallographic organization of the room-temperature 12Cr1MoV steel samples. Combined with metallographic analysis, preliminary analysis of the precipitated particles show that carbide particles precipitated from the tissue during the pearlite spheroidization process. Figure 3c shows the scan results of the energy spectrum analysis of the precipitated phase particles on the cracks along the crystal.

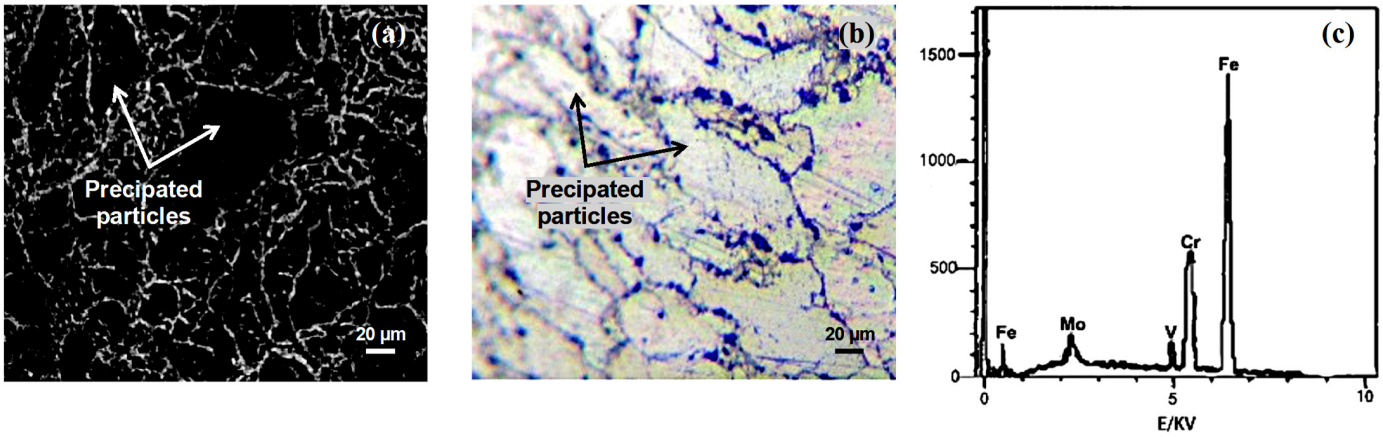

Figure 3. Microscopic views, (**a**,**b**), of carbide precipitation phase; (**c**) results of analytical phase energy spectroscopy.

These results indicate that the Cr, Mo, V, and other elements in Sample 2 are heavily precipitated in the grain boundaries and in the precipitated carbides that depleted Cr, Mo, V, and other elements in the matrix that play a solid solution role. This is corroborated by chemical composition test results on the metal tissue, which showed decreased Cr, Mo, and V contents.

These results indicate that, after 60,000 h of high-pressure, high-temperature use, pearlite and bainite disappear from the lamellar structure of the metal. At the same time, elements such as Cr and Mo also precipitate out of the tissue matrix in the form of carbides, along with some elements present in the ferrite. Most elements gradually spheroidize, grow along the grain boundaries, and decrease the solid-solution alloying element in the matrix. Migration of this alloy element significantly reduces the hardness and high-temperature properties of the metal.

3.3. Tensile Properties of Metals

Figure 4a shows the results of the room-temperature tensile performance tests. To reprise, the two samples are from 12Cr1MoV steel tubes designed for high-pressure, high temperature industrial use, whereas the test result for Sample 2, which has been used for 60,000 h is indicated in Figure 4b. The vertical comparisons for each mechanical test and corresponding results are also included in Table 2.

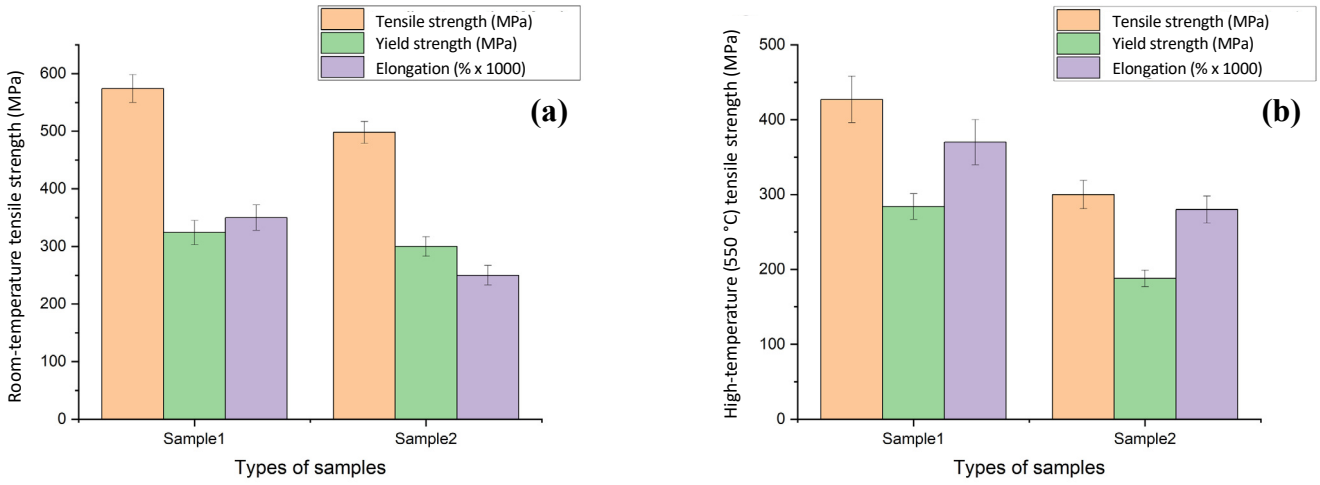

Figure 4. (**a**) Room-temperature tensile test, (**b**) high temperature tensile testing.

Table 2. Tensile test of Sample 1 and Sample 2 at room temperature and high temperature.

Sample/Temperature	Tensile Strength (MPa)	Yield Strength (MPa)	Elongation (% ×1000)
Sample 1 Room temperature	585.36	311.56	350.53
Sample 2 Room temperature	495.14	300.42	270.54
Sample 1 High temperature	423.65	290.53	384.68
Sample 2 High temperature	303.32	188.34	289.96

At room temperature, the GB5310-2008 standard for tensile strength range of 12Cr1MoV steel is 470–640 MPa, non-proportional elongation strength is no less than 255 MPa, and elongation after the break is no less than 21% as indicated in the upper sector of Table 2. Whereas, after 60,000 h of use, the room-temperature tensile strength and the specified non-proportional elongation strength of the steel samples reached 498 MPa and 300 MPa, respectively.

Comparing the room temperature tensile strength of Sample 1 with specified non-proportional elongation strength, Sample 2 data showed a significant decrease of 28.6% in elongation after the break. In other words, the plasticity of Sample 2 decreased significantly after 60,000 h of use.

Figure 4b summarizes the high-temperature (550 °C) tensile performance test results. For instance, at 550 °C, the high-temperature tensile strength and non-proportional elongation strength of 12Cr1MoV steel continue to decrease. Figure 4 also shows the average values and the ranges (maximum and minimum values) of variance of the coefficient of variation of the tensile and yield strength properties and the elongations. As documented in the lower sector of Table 2, the high-temperature tensile strength of Sample 2 is only 300 MPa while non-proportional elongation strength is 188 MPa.

The increase in elongation at break at high temperatures is due to the reduced hardness of 12Cr1MoV steel compared with its condition at room temperature. In other words, Sample 2 decreased in strength at room temperature as well as under high-temperature tensile tests. This decrease can be attributed to the deterioration of the organizational properties of the metal after long-term, high-temperature use, which leads to a decrease in strength [12,13].

3.4. Analysis of Impact Properties

The 12Cr1MoV samples were tested for long-term use at high temperatures from 530 °C to 550 °C, a temperature range that includes the tempering embrittlement temperature of 12Cr1MoV. In other words, in long-term high-temperature use, 12Cr1MoV steel undergoes tempering embrittlement. Figure 5 shows the impact test results of Sample 1 and Sample 2 at 0 °C and at 550 °C.

The impact test results of Sample 2 show that 12Cr1MoV steel becomes highly brittle after long-term, high-temperature use. For instance, each temperature shock work of Sample 2 (used 12Cr1MoV steel) is less than the absorbed shock work of Sample 1 (new 12Cr1MoV steel).

At the same time, the impact at 0 °C was lower by more than 40 J compared with the full-size impact energy absorption requirements of GB5310-2008 standard for 12Cr1MoV steel. In short, at 0 °C, 12Cr1MoV steel becomes brittle and extremely susceptible to cracking on impact.

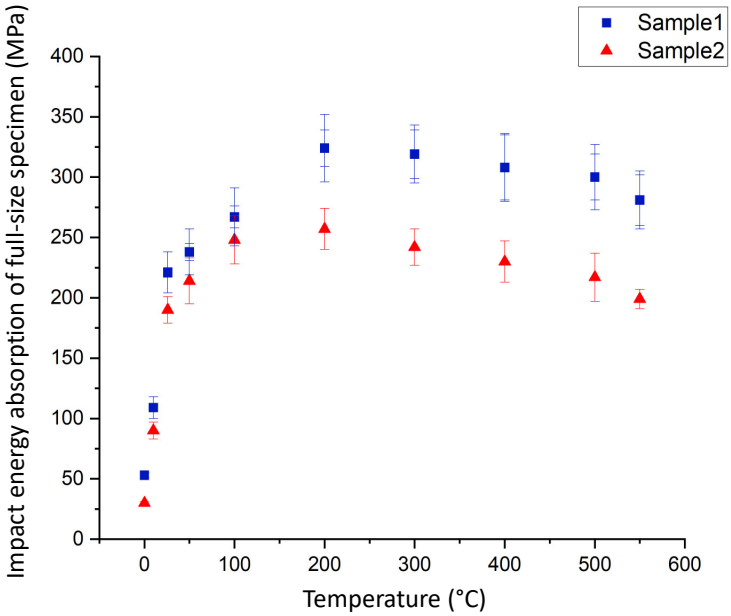

Figure 5. Impact test results of 12Cr1MoV steel from 0 °C to 550 °C.

3.5. Fracture Analysis

Figure 6 shows the fracture morphology of Sample 2 at room temperature. The SEM diagram indicates that the room temperature tensile fracture modes of 12Cr1MoV steel are penetrating crystal fractures that include ductile fracture, fiber area plastic fracture deformation, and inside cracks through the crystal. As well, there are stretched isometric nests of various sizes and unevenness within the fiber zone where the plastic deformation occurs. In addition, some precipitated phase particles form along the crystal cracks.

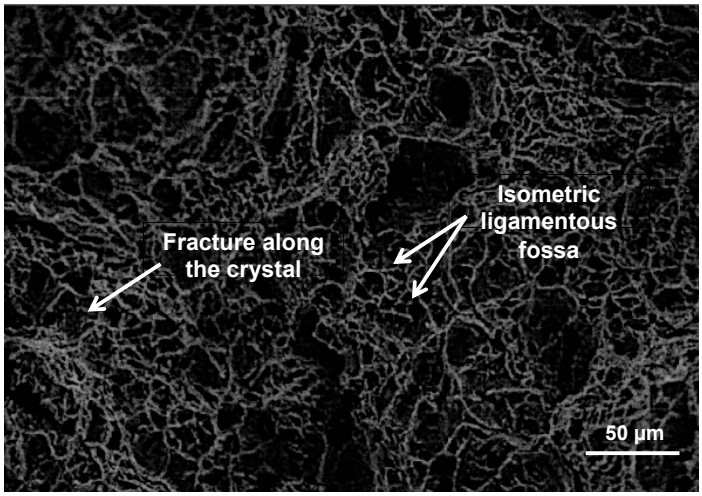

Figure 6. Fracture analysis of 12Cr1MoV steel at 60,000 h.

Metallographic analysis shows that precipitated carbides collect at the grain boundaries but do not cause tensile fractures along the grain boundaries during the non-impact loading tensile fracture process.

To reiterate, the precipitated carbides do not cause tensile fracture along the grain boundary; the fracture mode is through the grain fracture. The type of ligamentous fossa is isometric ligamentous fossa. At the same time, fiber zone fractures are in different sizes and include unevenly stretched isometric tough nests. This indicates that, after 60,000 h of use, the 12Cr1MoV steel sample remains ductile and shows good plasticity.

4. Discussion

12Cr1MoV steel is normalized and tempered at high temperatures, where its normal metal organization includes ferrite and pearlite (or local bainite). Compared with the same type of low-alloy pearlitic heat-resistant steel, 12Cr1MoV shows better processability and much higher thermal strength. [14] The alloy's thermal strength is achieved by adding solid solution elements to achieve solid solution strengthening, precipitation strengthening of carbides, and grain boundary strengthening.

One key mechanism for high-temperature strengthening of low-alloy, heat-resistant steel is the precipitation of thermodynamically stable carbide phases from solid solutions. Considering the strengthening mechanism from the dislocation mechanism of the metal tissue, the precipitation of thermodynamically stable carbides from the solid solution is more effective than solid solution strengthening [15–17]. However, the normal metallographic organization of 12Cr1MoV steel is without carbide precipitation. Thus, for 12Cr1MoV steel, a solid solution strengthening mechanism is the decisive factor in inducing thermal strength. For instance, it is generally believed that the impact on the thermal strength of the steel mainly depends on (a) the type and content of the added solid solution elements; (b) the degree of dispersion of the added solid solution elements, (c) the distribution of the added solid solution elements; and (d) their stability under long-term high-temperature stress [18].

After a period of high-temperature use, pearlite spheroidization and decomposition in 12Cr1MoV low-alloy, heat-resistant steel leads to the gradual precipitation of Cr, Mo, and other elements from the tissue matrix, forming carbide on the grain boundaries. This reduces the Cr, Mo, V, and other elements that provide the matrix with a solid solution.

The presence of carbide alters the nature of the grain boundaries. Carbide roughening as a microstructural parameter can be used to explore the high and complex non-linear relationships between various factors, with different microstructural images of carbide roughening in 12Cr1MoV steel samples at different high-temperature service times. For instance, after 60,000 h of use at 550 °C, 12Cr1MoV steel accumulates carbides in lamellar distribution on the grain boundaries. These lamellar carbides weaken the grain boundaries and lower the thermal strength of the metal. These carbides contain Cr and Mo elements that create cracks in the grain boundary as they cannot solidify the matrix organization at the grain boundaries. At the same time, these carbides form in the crystal, increase brittleness, and lower thermal strength in 12Cr1MoV steel [19].

The current standard approach to assessing the useful life of metallic materials is still based on a single material performance indicator. However, life assessment of metallic materials is a complex and comprehensive process that requires high accuracy. To help address this issue, this paper compares a new 12Cr1MoV steel sample with another 12Cr1MoV steel sample that has been subjected to 60,000 h at high temperature and high-pressure conditions. A comprehensive analysis of the mechanical properties of the 12Cr1MoV steel sample after operation at high temperature and pressure is presented, and the paper provides a way in which a model for assessing the remaining life of 12Cr1MoV steel can be developed through a large number of specific tests. This model can be very helpful when assessing the remaining life of 12Cr1MoV steel in practical engineering [20].

The goal of this study is to establish a theoretical model for the life assessment of 12Cr1MoV steel through analysis of the specific parameters so that life assessment of 12Cr1MoV steel under different conditions can be explored.

5. Conclusions

After 60,000 h of use, there is a gradual decrease in Cr, Mo, and V elements in the specimens of 12Cr1MoV steel. Long-term, high-temperature use of 12Cr1MoV steel significantly increases brittleness. As well, room temperature and high-temperature tensile test strength decrease. This is due to the spheroidization of pearlite, which precipitates carbides on the grain boundaries.

High-temperature use of 12Cr1MoV steel results in creep damage caused by carbide precipitation and reduction in alloy elements, both of which are important indicators in future analysis and evaluation of metal aging, which should focus on the size, quantity, density, and distribution of the carbides.

Carbide roughening as a microstructural parameter can be used to explore the high and complex non-linear relationships between various factors, with different microstructural images of carbide roughening in 12Cr1MoV steel samples at different high-temperature service times (between 0 h and 60,000 h). A new 12Cr1MoV metallographic cluster was analyzed using the area method to calculate the ferrite area fraction of the polished surface of the metallographic, 55–67%, the pearlite area fraction of 30–42%, and the original carbide and non-metallic inclusions area fraction of 3–4.7%. However, the area fraction of ferrite rose to 80–89%, the area fraction of pearlite was only 10–12%, and the area fraction of carbide rose to 7–12% in the metallographic cluster of aging 12Cr1MoV after 60,000 h of operation.

Author Contributions: Conceptualization, J.L. and Y.L.; methodology, J.L. and Y.L.; formal analysis, J.L. and Y.L.; writing—original draft preparation, J.L.; writing—review and editing, J.L. and Y.L.; visualization, J.L. and Y.L.; supervision, Y.L.; project administration, Y.L. All authors have read and agreed to the published version of the manuscript.

Funding: This research received no external funding.

Institutional Review Board Statement: Not applicable.

Informed Consent Statement: Not applicable.

Data Availability Statement: All data related to this study are publicly available upon reasonable request to the corresponding author.

Conflicts of Interest: The authors declare no conflict of interest.

References

1. Le, Y. Overview and Development of Steel for Power Station Boilers in the Former Soviet Union (1–3). 1992.
2. Du, Y.; Zhu, M.-L.; Liu, X.; Xuan, F.-Z. Effect of long-term aging on near-threshold fatigue crack growth of Ni–Cr–Mo–V steel welds. *J. Mater. Process. Technol.* **2015**, *226*, 228–237. [CrossRef]
3. Rao, R.; Kalyankar, V.D. Experimental investigation on submerged arc welding of Cr–Mo–V steel. *J. Adv. Manuf. Technol.* **2013**, *69*, 93–106. [CrossRef]
4. Zi, L.; Chun, L.; Ding, J.; Zhang, H. Characterization and Modelling of High Temperature Flow Behaviour of V Modified 2.25Cr-1Mo Heat Resistant Steel Plate. *J. Wuhan Univ. Technol. Mater. Sci. Ed.* **2020**, *35*, 192–199.
5. Shen, Y.; Zheng, G.; Wang, C. Evolution of Soft Zone in a Simulated 1.25Cr-0.5Mo Steel-Welded Joint During Post-weld Heat Treatment. *Metall. Mater. Trans. A* **2021**, *52*, 1581–1587. [CrossRef]
6. Bocchi, S.; Cabrini, M.; D'Urso, G.; Giardini, C.; Lorenzi, S.; Pastore, T. Stress enhanced intergranular corrosion of friction stir welded AA2024-T3. *Eng. Fail. Anal.* **2020**, *111*, 104483. [CrossRef]
7. Liu, H. Performance of heat-resistant steel P92 used in 1000 MW ultra-supercritical unit after long-term service at high temperature. *Trans. Mater. Heat Treat.* **2012**, *33*, 105–110.
8. Cattivelli, A.; Roy, M.J.; Burke, M.G.; Dhers, J.; Lee, T.L.; Francis, J.A. Internal stresses in a clad pressure vessel steel during post weld heat treatment and their relevance to underclad cracking. *Int. J. Press. Vessel. Pip.* **2021**, *193*, 104448. [CrossRef]
9. Zhang, Z.; Fan, J.; Li, R.; Kou, H.; Chen, Z.; Wang, Q.; Zhang, H.; Wang, J.; Gao, Q.; Li, J. Orientation dependent behavior of tensile-creep deformation of hot rolled Ti65 titanium alloy sheet. *J. Mater. Sci. Technol.* **2021**, *75*, 265–275. [CrossRef]
10. Zhang, Y.; Cheng, S.; Wu, S.; Cheng, F. The evolution of microstructure and intergranular corrosion resistance of duplex stainless-steel joint in multi-pass welding. *J. Mater. Process Technol.* **2020**, *277*, 116471. [CrossRef]
11. Tang, P.; Huang, S.; Tian, W.; Ling, Z.; Jin, N.; Li, F. Residual life evaluation of 12Cr1MoVG steel for main steam pipeline. *IOP Conf. Ser. Earth Environ. Sci.* **2021**, *675*, 012193. [CrossRef]
12. Purbolaksono, J.; Ahmad, J.; Beng, L.C.; Rashid, A.Z.; Khinani, A.; Ali, A.A. Failure analysis on a primary superheater tube of a power plant. *Eng. Fail. Anal.* **2010**, *17*, 158–167. [CrossRef]
13. Tokaji, K.; Horie, T.; Enomoto, Y. Effects of microstructure and carbide spheroidization on fatigue behaviour in high V-Cr-Ni cast irons. *Int. J. Fatigue* **2006**, *28*, 281–288. [CrossRef]
14. Yan, J.; Hui, D.; Hai, B.; Cong, F.; Fan, L. In-situ investigation of tensile deformation and fracture mechanism of 12Cr1MoV steel after long-term service. *Mater. Sci. Eng. A* **2017**, *700*, 33–41. [CrossRef]

15. Alsagabi, S.; Shrestha, T.; Charit, I. High temperature tensile deformation behavior of Grade 92 steel. *J. Nucl. Mater.* **2014**, *453*, 151–157. [CrossRef]
16. Wang, Z.; Yu, H.; Wang, Z. A local mesh replacement method for modeling near-interfacial crack growth in 2D composite structures. *Theor. Appl. Mech.* **2015**, *75*, 70–77. [CrossRef]
17. Sadrmomtazi, A.; Lotfi-Omran, O.M.; Nikbin, I. Influence of cement content and maximum aggregate size on the fracture parameters of magnetite concrete using WFM, SEM and BEM. *Theor. Appl. Fract. Mech.* **2020**, *107*, 102482. [CrossRef]
18. Liu, Z.; Hu, X.; Yang, Z.; Yang, B.; Chen, J.; Luo, Y.; Song, M. Optimization Study of Post-Weld Heat Treatment for 12Cr1MoV Pipe Welded Joint. *Metals* **2021**, *1*, 127. [CrossRef]
19. Cao, F.; Li, J.; Hou, W.; Shen, Y.; Ni, R. Microstructural evolution and mechanical properties of the friction stir welded Al[S]Cu dissimilar joint enhanced by post-weld heat treatment. *Mater. Charact.* **2021**, *174*, 110998. [CrossRef]
20. da Silva Lima, C.; Verdier, M.; Robaut, F.; Ghanbaja, J.; Badinier, G.; Marlaud, T.; Tassin, C.; Van Landeghem, H.P. Evolution of a low-alloy steel/nickel superalloy dissimilar metal weld during post-weld heat treatment. *Weld. World* **2021**, *65*, 1871–1885. [CrossRef]